www.czasopisma.pan.pl PAN www.journals.pan.pl

GEODESY AND CARTOGRAPHY
Vol. 69, No. 1, 2020, pp. 85–96

DOI: https://doi.org/10.24425/gac.2020.131079

Research paper

Monitoring of displacements and deformations of the earth's surface near the Stebnyk city using radar images of Sentinel-1

Ihor Trevoho[1]*, Borys Chetverikov[2], Lubov Babiy[3], Mariia Malanchuk[4]

[1]Lviv Polytechnic National University, Department of Geodesy,
12 S. Bandery St. Lviv, Ukraine 79013
e-mail: itrevoho@gmail.com, ORCID: http://orcid.org/0000-0002-2368-9088

[2,3]Lviv Polytechnic National University, Department of Photogrammetry and Geoinformatics,
12 S. Bandery St. Lviv, Ukraine, 79013
[2]e-mail: chetverikov@email.ua, ORCID: http://orcid.org/0000-0001-5187-008X
[3]e-mail: lbabiy@i.ua, ORCID: http://orcid.org/0000-0002-5772-4865

[4] Lviv Polytechnic National University, Department of Cadastre of Territiry,
12 S. Bandery St. Lviv, Ukraine, 79013
e-mail: malanchuk.mari@gmail.com, ORCID: http://orcid.org/0000-0003-0819-6573

*Corresponding author: Ihor Trevoho

Received: 5 February 2020 / Accepted: 2 April 2020

Abstract: This article applies radar interferometry technologies implemented in the ENVI SARscape and SNAP software environment provided by the processing of data from the Sentinel-1 satellite. The study was carried out based on six radar images of Sentinel-1A and Sentinel -1B taken from September 2017 until February 2018 with an interval of one month and on the radar-module of the already mentioned SNAP software. The main input data for solving the considered problem are radar images received from the satellite Sentinel-1B on the territory of Stebnyk-Truskavets for six months with an interval of one month. Monitoring of the Earth's surface using radar data of the Sentinel-1A with a synthesized aperture is implemented with the application of interferometric methods of Persistent Scatterers and Small baselines interferometry for estimating small displacements of the Earth's surface and structures. The obtained quantitative and qualitative indicators of monitoring do not answer the processes that take place and lead to vertical displacements the six months but do provide an opportunity to assess the extent and trends of their development. The specification in each case can be accomplished by ground methods, which greatly simplify the search for sites with critical parameters of vertical displacements which can have negative consequences and lead to an emergency.

Keywords: radar interferometry; Synthetic Aperture Radar; Sentinel-1; deformations of the Earth's surface

1. Introduction

In recent years there is a tendency to increase the number of radar systems for remote sensing of the Earth's surface with a high spatial resolution (1–8 m). This is explained by many advantages: the ability to take an image at any time of day independently of cloud cover, the high penetrating ability of radar radiation, and application of different states of the polarization ellipse. However, the more sophisticated side-view technology and coherent radiation require fundamentally different methods and a different data-processing algorithm than used for the optical wave range. In practice, Persistent Scatterers Interferometry and Small Baselines Series Interferometry realized in the SARscape software are used to solve problems of space radar monitoring of landslides and deformations of the Earth's surface and structures. Satellite interferometric radars work with different resolutions, in different wavelength ranges and with different frequencies of the survey for the same territory. Atmospheric and ionospheric interference, vegetation, and snow cover also influence survey results. Interferometric data are stored in archives and can be purchased from space agencies (satellite owners). The ability to use archival data is a considerable advantage of satellite interferometry since it allows exploring not only modern deformations but also deformations over long periods.

On September 30, 2017, near the towns Drohobych and Truskavets (Ukraine), an earthquake happened. Thereupon in the territory of LLC "Polymineral", a huge natural crater with a diameter of about 300 m and depth up to 50m opened, and it can increase. Another 50 meters of this site can subside (Figure 1). The location of the crater is located over the former salt mines, which are not currently operating. Within many decades, potash salt was extracted here until the early 2000s. As a result, huge underground caverns remained. In 2004 a project for conservation of the mines was developed, but it had not been implemented.

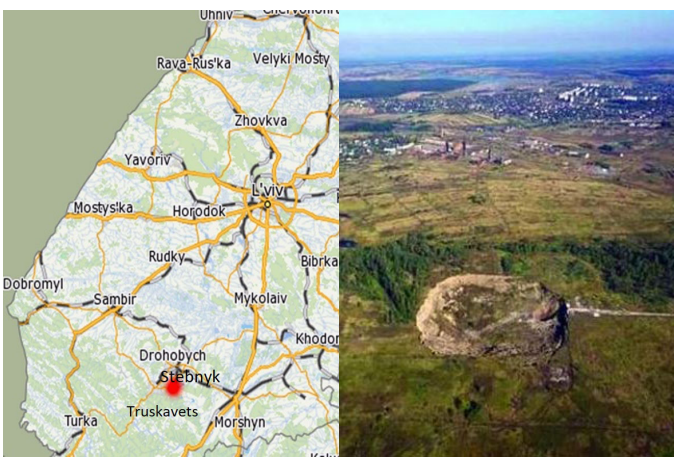

Fig. 1. The surface deformation caused by natural crater near Truskavets and Stebnyk, Lviv regions

There are many methods of studying this type of disaster, both terrestrial and remote. One of the most effective remote methods is the application of radar interferometry.

Many methods exist for the detection and measurement of ground subsidence. Radar interferometry is the most effective method. Therefore, this work aims to determine the changes of the natural crater on the Earth's surface near the city of Stebnyk (Ukraine) for a half-year period using space radar images received from the satellite Sentinel-1A.

A large group of scientists, mostly from Western Europe, the USA, Canada, Japan, and less from Russia and Kazakhstan, Ukraine was studying the application of radar interferometry to determine the displacement of the Earth's surface. Many scientists have been engaged in the development of theoretical foundations of interferometry. Notable is the scientific works published since the early '70s of the last century. Recent works include (Berardino et al., 2002; Ferretti et al., 2001; Rosen et al., 2000; Papathanassiou and Cloude, 2001). The scope of radar interferometry was significantly expanded after the development of various modifications of the method of persistent scatterers. The basic idea is the identification of image pixels contained in so-called persistent scatterers (Ferretti, 2000). If, as it is usually the case, the dimensions of persistent scatterers do not exceed the dimensions of the resolution element, then the value of coherence is acceptable even for those interferograms for which the interferometer base is close to the critical value. Besides, the entire available set of images can be included in the interferometric calculations. The identification of persistent scatterers allows us to assess atmospheric impediments and eliminate them from differential interferograms, which increases the accuracy of estimations of landslides on the Earth's surface. In Feretti's method, persistent scatterers are distinguished by the results of the analysis of the behavior of scattering sites in time.

In Hooper et al. (2004) a method for analyzing the distribution of persistent scatterers over space is proposed. This method is independent of how the rate of landslide changes over time. Later, the method of small baselines was developed. The idea of the method is close to Hooper's approach and is based on finding such scattering sites, in which the influence of decorrelation and noises is minimal. For such pixels, the separation of phase associated with phase deformations arising as a result of atmospheric interference and inaccuracies in DEM is performed.

A large number of projects were presented regarding the application of interferometric technology for measuring landslides of the Earth's surface. In this sphere, there are the trends of joint analysis of radar data from different satellites in order to increase the volume of analyzed data, to obtain a more complete and accurate picture of deformations, and to perform a retrospective analysis (Chen et al., 2016; Haghshenas Haghighi et al., 2016). Interferometric processing is performed applying SBas and PS methods using the software Gamma, Doris, SARscape, StamPS, and Sentinel-1 Toolbox. The control of the obtained results is based on observations from the ground (Garthwaite et al., 2015). Great attention is paid to technologies and methods of using space radar data in systems for monitoring of natural and anthropogenic objects and prevention and elimination of the consequences of natural disasters accompanied by landslides of the Earth's surface that include landslides, volcanic eruptions, earthquakes, and floods. The methods of radar interferometry are most widely used in the study of geodynamic phenomena and deformations of structures (Meyer et al., 2015; Floyd et al., 2014). Search and mapping of surface changes are performed based on the analysis of both phase and amplitude layer

of radar data (Ajadi et al., 2016). Solving the problem of using the radar interferometry method to determine landscape changes has been considered in (Mora et al., 2003; Treuhaft and Siqueira, 2000; Feranec et al., 2007). The method of radar interferometry is used for the study of forest cover (Garestier et al., 2008; Lee et al., 2009).

Since our task is to determine the changes in the relief of the Earth's surface caused by its subsidence, we are particularly interested in the works (Schneider et al., 2006; Livingstone et al., 2002; Colesanti et al., 2003; Lanari et al., 2004), which describe the application of radar interferometry namely for deformation processes and creation of digital elevation models.

2. Main concepts of radar interferometry

The quality of the results of interferometric processing directly depends on the value of the perpendicular component of the baseline. On the one hand, the quality of the map of displacements of the Earth surface obtained by the interferometric method can be improved by decreasing the length of the perpendicular baseline. In the case when the baseline is equal to zero, the interferogram, calculated on such a pair of images, generally contains only the phase of displacement. On the other hand, when exceeding a specific critical value of the baseline, interferometric processing becomes in principle impossible due to spatial decorrelation (Lachaise et al., 2012; Krieger. et al., 2010; Fritz et al., 2011; Belcher, 2008).

The critical value of the perpendicular spatial baseline for each pair of images can be calculated using the following formula:

$$B_{n,cr} = \frac{\lambda R \tan(\theta)}{2R_r}, \tag{1}$$

where: $B_{n,cr}$ is the critical baseline; λ is the length of the radar sensor wave; R_r is the spatial resolution in the direction of the slant range.

According to this formula, the critical perpendicular baseline for the ENVISAT ASAR Image Mode data is about 900–1500 m, and for ALOS – PALSAR data is about 6500 m in FBS mode and 13,000 m in FBD mode (6500 m when cross-processing of FBS and FBD modes). The optimal perpendicular baseline for calculating displacements in the case of both the above-mentioned satellites ranges from 0 to 30% of the critical baseline. The interval of time between acquisitions of images that make up an interferometric pair is called the temporal baseline. The concept of a temporary baseline is directly related to such an essential problem as temporary decorrelation which occurs due to changes in the relief, vegetation, humidity and other properties that reflect the radar beam on the surface that occurred during the period between the image acquisitions. The problem of temporal decorrelation can be solved by increasing the wavelength (which increases the "penetrating" power of the waves) or the reduction of the temporal baseline, i.e., the interval between the image acquisitions. During the monitoring of the Earth surface displacements, we apply the abovementioned approach of interferometric processing of image pairs selected according to the principle of the smallest baselines

from all possible image pairs. Based on that, the processing result was presented in the form of displacement maps for the periods between the first image acquisition and each subsequent image acquisition, one after the other. That is, the result shows the development of the displacements in time, as well as the final map of displacements for the entire period of observations.

In addition to the spatial and temporal baselines, the difference in the positions of the Doppler centroid of the Earth's rotation for a pair of images is an important parameter that determines the possibility or impossibility of interferometric processing. All processed pairs are characterized by low or average values of this parameter, which has a positive effect on the processing. If the values of the spatial and temporal baselines, as well as the difference in the positions of the Doppler centroid, allows interferometric processing, then it is possible to calculate the interferogram. Each radar image of the interferometric pair contains an amplitude and phase layers. The amplitude layer is more suitable for visual analysis. The resulting phase F, obtained during interferometric processing of phase layers of interferometric image pair, generally consists of the following components:

$$F = F_{topo} + F_{def} + F_{atm} + F_n \tag{2}$$

where: F_{topo} is the phase shift component due to observation of the topography with two different angles; F_{def} is the phase shift component due to the displacement of the reflective surface between image acquisitions; F_{atm} is the phase shift component due to the difference of lengths of the line of sight caused by refraction; F_n is the phase variation due to electromagnetic noise.

The last two components do not carry information about the topography of the surface. Therefore, with the help of correction and filtering, they are excluded.

$$F_{topo} = -\frac{4\pi B_{\perp}}{\lambda r \sin\Theta} z + F_{flat\_earth}\,, \tag{3}$$

where: $B_{\perp}$ is the perpendicular component of the baseline, which connects the position of the satellite during reacquisition of a specific point of the Earth's surface; Θ is the angle of view of the surface during the first pass; λ is the wavelength of scanning irradiation; r is the distance between the antenna and the point on the surface; z is the height of the surface over the reference ellipsoid; F_{flat_earth} is the determined phase, calculated from the model of the reference ellipsoid.

Removal of the obstructive component F_{flat_earth} is necessary to reduce the high-frequency phase transitions that arise on the interferogram due to the difference of distance the signal passes when acquiring images from different positions, as well as changes caused by the relief of the surface. Information for calculating F_{flat_earth} can be a digital low-resolution relief model, for which we can use GTOPO30 CMS (Global 30-Arc-Second digital elevation model) or digitized topographic maps of scale 1 : 100 000, 1 : 200 000. The size of the pixel of GTOPO30 is about 500 m for the middle latitudes, the inaccuracy of the referencing and distortion in the matching of separate parts of the maps make this relief rough and can spoil the interferometric phase. Vectorization of isolines and height points on topographic maps and further interpolation in order to obtain

a homogeneous grid (smoothing) is a rather laborious process that increases the time of DEM creation. During the processing of interferometric data of different satellites, it has been established that the best variant of the reference relief is the surface with constant height, the value of which is calculated as the average from the GTOPO30 DEM onto the area covered by the radar image. During the interferometric data processing of different satellites, it has been established that the best variant of the reference relief is the surface with constant height, the value of which is calculated as the average of the GTOPO30 DEM on the area covered by the radar image. In this case, there are no unreasonable sharp bursts of the phase, and the residual uncertainties caused by the registration range of the phase of the reflected signal from 0 to 2π are eliminated at the stage of phase unwrapping.

The value of the Earth's surface displacement Δr, which occurs during the time between repeated acquisitions is reflected in phase component F_{def}

$$F_{def} = \frac{4\pi}{\lambda}\Delta r. \tag{4}$$

From equations (2)–(4), it follows that the interferometric phase F contains information on both the relief and the displacement. At this F_{topo} manifests itself, the more significant the higher the value $B_{\perp}$ is, i.e., the further the satellite is in its re-pass from the first position.

Interferometric processing of a pair of images generally consists of a few primary stages (Figure 2).

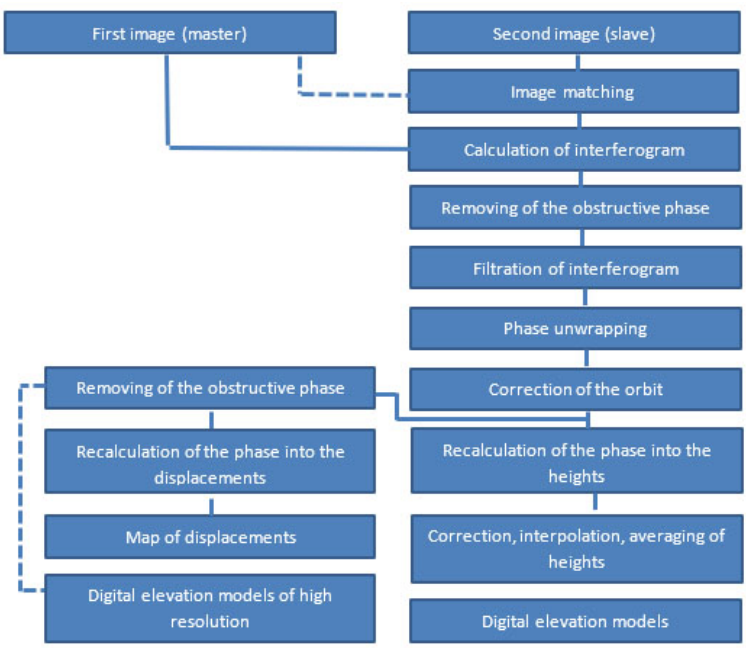

Fig. 2. Stages of interferometric processing

3. The method of determining the deformation of the earth's surface by radar images

Scientists from the Institute of geodesy of Lviv Polytechnic National University have been researching the monitoring of the vertical displacements on the natural crater near Truskavets and Stebnyk cities. The researches were implemented using the GNSS survey, accompanied by the application of inclinometers (Petrov, 2019). The researches had started in six months after the creation of the natural crater and are continuing up to now. For the second six months period, the value of subsidence determined by these geodetic methods was near 20 cm that indicates a decrease in vertical displacements comparing with our researches. We have decided to fill the first half-year gap with radar interferometry data.

The primary input data for solving the considered problem are radar images received from the satellite Sentinel-1B on the territory of Stebnyk-Truskavets for the six months with an interval of one month, namely: 04.10.2017, 27.10.2017, 14.11.2017, 21.12. 2017, and 23.1.2018, 26.2.2018. These images are acquired in the C-range with polarization VV+VH and Interferometric Wideswath (IW) survey mode. In this case, the swath of each image is 250 km.

Sentinel-1A images are available in three processing levels: Level-0, Level-1, Level-2. Our input data is of the first processing level. Level-1 data are the generally available products intended for most data users. Level-1 products are produced as Single Look Complex (SLC) and Ground Range Detected (GRD). Level-1 SLC products consist of focused SAR data geo-referenced using orbit and attitude data from the satellite and provided in zero-Doppler slant-range geometry. The products include a single look in each dimension using the full transmit signal bandwidth and consist of complex samples preserving the phase information. Interferometric processing of radar images is performed with special software (Fig. 2). Today leaders are the SARscape and Gamma software products. These are full-featured software products that contain a set of tools for performing all significant stages of radar data processing. The main difficulty is since this software is commercial, which limits the possibility of its use in low-budget projects. Alternatively, free software is available. DORIS and SNAP (Sentinel-1 Toolbox) are among the most popular products. These software products have the essential ability to process radar images, while there are certain limitations in the set of functions.

In our study, we use the software ENVI SARscape and SNAP for the processing of radar images. We select the main image, which is automatically co-registered (mutually identified) with all other images of the interferometric series. The accuracy is up to 1/100 of a pixel. The images (Source Product) are selected – menu Read, Read (2) at the stage of co-registration. Then subwath and bursts are selected, which should be the same for both images. We have selected the following pairs: 04.10.2017 and 27.10.2017, 27.10.2017 and 14.11.2017, 14.11.2017 and 21.12.2017, 21.12.2017 and 23.01.2018, 23.01.2018 and 26.02.2018 to estimate the dynamics of deformations of the Earth's surface, and the pair 27.10.2017 and 26.02.2018 to estimate how the surface was deformed for the period of half a year from the beginning of deformation. Since in our case, we are interested only in the six months before the beginning of the geodetic monitoring and

using Sentinel images, we can obtain an accuracy not exceeding the wavelength, and then we consider that it is sufficient to use six images to obtain displacement data for the six months.

4. Results

The processing of each pair is done in semi-automatic mode with the following four steps:

1. Automatic co-registration, calculation of interferogram, synthesis of a phase of relief, removing the obstructive phase from an interferogram, filtering of the differential interferogram, calculation of coherence, phase unwrapping.
2. Collection of points with known coordinates and heights for correction of orbital parameters.
3. Calculation of corrected differential interferograms and unwrapped phases.
4. Inversion of the obtained cross-time unwrapped phases with the restoration of consecutive in time history of the displacements. At the same time, as a result, the chronology of displacements from the first image of the series to the last is restored.

After analyzing the differential interferograms obtained during processing, there were indicated the sites created trough subsidences.

These trough subsidences of the Earth's surface are located in the area of the natural crater formation near Stebnyk city (Figure 3).

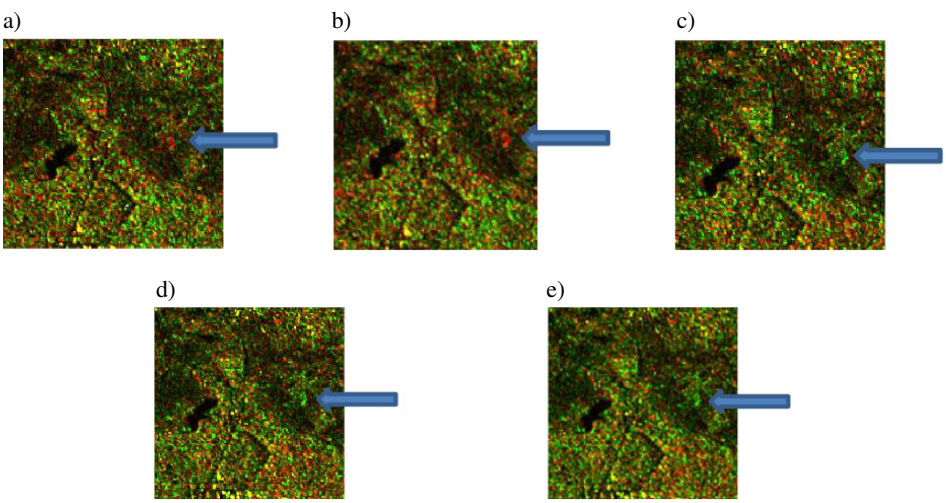

Fig. 3. Interferogram of the time-period: a) 04.10.2017–27.10.2017; b) 27.10.2017–14.11.2017; c) 14.11.2017–21.12.2017; d) 21.12.2017–23.01.2018; e) 23.01.2018–26.02.2018

Calculation of displacements with menu Phase to Displacement is implemented by the formula (5):

$$\Delta R = -\lambda 4\pi\phi_{diff} \tag{5}$$

and represents LOS-displacement, taken with a minus sign and measured in meters.

Calculation of vertical displacements by unwrapped interferogram includes the following steps (Figure 4):

1. Creation of a new band with the formula for calculating landslides.
2. Removing from it the area with low coherence.
3. Selection of the points that are immobile and determination of the value of their height.
4. Calculation of the value of this height from all points of the image.

Fig. 4. Vertical displacements on the crater near Stebnyk

The next step is to create a new band, in which one must enter the vertical displacement equation:

$$\frac{\Phi \cdot \lambda}{4 \cdot \pi \cdot \cos(\alpha)}, \tag{6}$$

where Φ is an unwrapping phase; λ is the wavelength, cm; α is an incident angle.

The unwrapping phase is the name of the band with an unwrapped interferogram of the current product. For Sentinel-1, the length of a wave is 5.55 cm. The incident angle is taken from Tie-Point Grids. The result is a vertical displacement in centimeters. After that, it is necessary to delete areas of low coherence. The limit value of coherence varies and starts at about 0.3. Now we have a relative vertical displacement between the two images.

According to the results of the implemented research, it was determined that the vertical deformation of the Earth's surface within the limits of the formed natural crater near the town of Stebnyk in the period from 04.10.2017 to 26.02.2018 is 29 cm in total. More detailed land subsidence in the studied periods is given in Table 1.

Table 1. Subsidence of the Earth's surface within the natural crater near the town of Stebnyk

	Subsidence of the Earth's surface				
	04.10.2017–27.10.2017	27.10.2017–14.11.2017	14.11.2017–21.12.2017	21.12.2017–23.01.2018	23.01.2018–26.02.2018
A quantitative index of subsidence (cm)	7 (7 days since event)	6 (13 days since event)	6 (19 days since event)	5 (24 days since event)	5 (29 days since event)

As seen from the obtained information, the largest vertical displacements within the natural crater were observed in the first months after the disaster and were 7 cm and

6 cm. In the last study period, the displacement was 5 cm. It can be assumed that the vertical displacements will decay if the seismic activity will not be observed in this area.

Using the results of the monitoring for the half-year period, the map of vertical displacements was created. As the area of the researched site is rather small in the limits of Sentinel image parameters, the map of vertical displacements was edited in the software Surfer for better representation. The scale of displacements is shown in centimetres and has a range of 7 cm at the start of the study and up to 29 cm in the last month of research. The map shows that the largest vertical displacements occurred in the northwest and southeast parts of the natural crater.

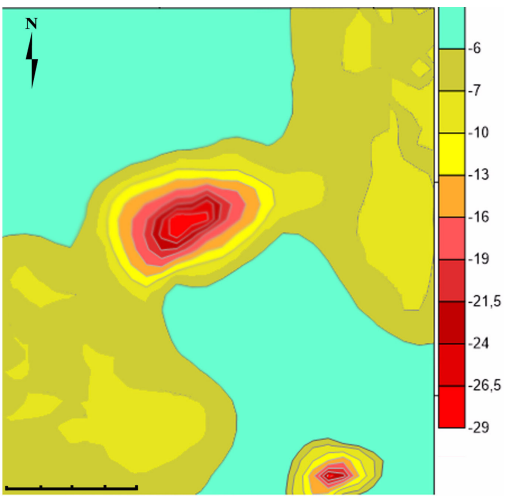

Fig. 5. Vertical displacement map or the research area from 04.10.2017 to 26.02.2018 (cm)

5. Conclusions

The obtained quantitative and qualitative indicators of monitoring do not answer the processes that take place and lead to vertical displacements but provide an opportunity to assess the extent and trends of their development. The specification in each case can be accomplished by ground methods, which significantly simplifies the search for places with critical parameters of vertical displacements, which can have negative consequences and lead to an emergency.

The possibility of all-weather space monitoring of large territories using free space information will significantly save public funds and will enable the creation of an effective system for preventing emergencies.

Acknowledgment

The manuscript does not have external founds.

References

Ajadi, O., Meyer, F. and Webley, P. (2016). Change detection in synthetic aperture radar images using a multiscale-driven approach. *Remote Sensing,* 8(6), 482. DOI: https://doi.org/10.3390/rs8060482.

Berardino, P., Fornaro, G., Lanari, R. and Sansosti, E. (2002). A new algorithm for surface deformation monitoring based on small baseline differential SAR interferograms. *IEEE Transactions on geoscience and remote sensing*, 40(11), 2375–2383. DOI: 10.1109/TGRS.2002.803792.

Belcher, D.P. (2008). Theoretical limits on SAR imposed by the ionosphere. *IET Radar, Sonar & Navigation*, 2(6), 435–448.

Chen, M., Tomás, R., Li, Z., Motagh, M., Li, T., Hu, L. and Gong, X. (2016). Imaging land subsidence induced by groundwater extraction in Beijing (China) using satellite radar interferometry. *Remote Sensing*, 8(6), 468. DOI: 10.3390/rs8060468.

Colesanti, C., Ferretti, A., Novali, F., Prati, C. and Rocca, F. (2003). SAR monitoring of progressive and seasonal ground deformation using the permanent scatterers technique. *IEEE Transactions on Geoscience and Remote Sensing*, 41(7), 1685–1701. DOI: 10.1109/TGRS.2003.813278.

Feranec, J., Hazeu, G., Christensen, S. and Jaffrain, G. (2007). Corine land cover change detection in Europe (case studies of the Netherlands and Slovakia). *Land use policy* 24(1), 234–247.

Ferretti, A., Prati, C., and Rocca, F. (1999). Permanent scatterers in SAR interferometry. *IEEE Transactions on Geoscience and Remote Sensing*, 39(1), 8–20. DOI: 10.1109/36.898661.

Ferretti, A., Prati C. and Rocca F. (2001). Permanent scatterers in SAR interferometry. *IEEE Transactions on Geoscience and Remote Sensing*, 39(1), 8–20. DOI: 10.1109/36.898661.

Ferretti, A., Prati, C. and Rocca, F. (2000). Nonlinear subsidence rate estimation using permanent scatterers in differential SAR interferometry. *IEEE Transactions on Geoscience and Remote Sensing*, 38(5), 2202–2212. DOI: 10.1109/36.868878.

Floyd, A.L., Prakash, A., Meyer, F.J., Gens, R. and Liljedahl, A. (2014). Using synthetic aperture radar to define spring breakup on the Kuparuk river, Northern Alaska. *Arctic*, 67(4), 462–471. DOI: 10.14430/arctic4426.

Fritz, T., Rossi, C., Yague-Martinez, N., Rodriguez-Gonzalez, F., Lachaise, M. and Breit, H. (2011). Interferometric processing of TanDEM-X data. In *2011 IEEE International Geoscience and Remote Sensing Symposium*, 2011 (pp. 2428–2431). Vancouver, Canada: IEEE.

Garestier, F., Dubois-Fernandez, P. C. and Champion, I. (2008). Forest height inversion using high-resolution P-band Pol-InSAR data. *IEEE Transactions on Geoscience and Remote Sensing*, 46(11), 3544–3559. DOI: 10.1109/TGRS.2008.922032.

Garthwaite, M.C., Nancarrow, S., Hislop, A., Thankappan, M., Dawson, J.H. and Lawrie, S. (2015). The Design of Radar Corner Reflectors for the Australian Geophysical Observing System: A single design suitable for InSAR deformation monitoring and SAR calibration at multiple microwave frequency bands. Canberra, Australia: Geoscience Australia.

Haghshenas Haghighi, M. and Motagh, M. (2016). Assessment of ground surface displacement in Taihape landslide, New Zealand, with C-and X-band SAR interferometry. *New Zealand Journal of Geology and Geophysics*, 59(1), 136–146. DOI: 10.1080/00288306.2015.1127824.

Hooper, A., Zebker, H., Segall, P. and Kampes, B. (2004). A new method for measuring deformation on volcanoes and other natural terrains using InSAR persistent scatterers. *Geophysical Research Letters*, 31(23), 1–5. DOI: 10.1029/2004GL021737.

Krieger, G., Hajnsek, I., Papathanassiou, K.P., Younis, M. and Moreira, A. (2010). Interferometric synthetic aperture radar (SAR) missions employing formation flying. *Proceedings of the IEEE*, 98(5), 816–843. DOI: 10.1109/JPROC.2009.2038948.

Lanari, R., Mora, O., Manunta, M., Mallorquí, J.J., Berardino, P. and Sansosti, E. (2004). A small-baseline approach for investigating deformations on full-resolution differential SAR interferograms. *IEEE Transactions on Geoscience and Remote Sensing*, 42(7), 1377–1386. DOI: 10.1109/TGRS.2004.828196.

Lachaise, M., Balss, U., Fritz, T. and Breit, H. (2012, July). The dual-baseline interferometric processing chain for the TanDEM-X mission. In *IEEE International Geoscience and Remote Sensing Symposium, 2012* (pp. 5562–5565). Munich, Germany: IEEE.

Lee, S.K., Kugler, F., Hajnsek, I. and Papathanassiou, K.P. (2009, January). The impact of temporal decorrelation over forest terrain in polarimetric SAR interferometry. Proceedings of the Fourth International Workshop on Science and Applications of SAR Polarimetry and Polarimetric Interferometry PolInSAR 2009. ISBN:978-92-9221-232-2. Noordwijk, Netherlands: European Space Agency.

Livingstone, C.E., Sikaneta, I., Gierull, C.H., Chiu, S., Beaudoin, A., Campbell, J. and Knight, T.A. (2002). An airborne synthetic aperture radar (SAR) experiment to support RADARSAT-2 ground moving target indication (GMTI). *Canadian Journal of Remote Sensing*, 28(6), 794–813. DOI: 10.5589/m02-074.

Meyer, F.J., McAlpin, D.B., Gong, W., Ajadi, O., Arko, S., Webley, P.W. and Dehn, J. (2015). Integrating SAR and derived products into operational volcano monitoring and decision support systems. *ISPRS Journal of Photogrammetry and Remote Sensing*, 100, 106–117.

Mora, O., Mallorqui, J.J. and Broquetas, A. (2003). Linear and nonlinear terrain deformation maps from a reduced set of interferometric SAR images. *IEEE Transactions on Geoscience and Remote Sensing*, 41(10), 2243–2253. DOI: 10.1109/TGRS.2003.814657.

Papathanassiou, K.P. and Cloude, S.R. (2001). Single-baseline polarimetric SAR interferometry. *IEEE Transactions on Geoscience and Remote Sensing*, 39(11), 2352–2363. DOI: 10.1109/36.964971.

Petrov, S.L. (2019). Monitoring of vertical displacements of technogenically loaded territories by geodetic methods. Author's abstract of candidate's thesis. Lviv. 26 p. (Ukrainian).

Rosen, P.A., Hensley, S., Joughin, I.R., Li, F.K., Madsen, S.N., Rodriguez, E. and Goldstein, R.M. (2000). Synthetic aperture radar interferometry. *Proceedings of the IEEE*, 88(3), 333–382.

Treuhaft, R.N. and Siqueira, P.R. (2000). Vertical structure of vegetated land surfaces from interferometric and polarimetric radar. *Radio Science*, 35(1), 141–177.

Zandona-Schneider, R., Papathanassiou, K.P., Hajnsek, I. and Moreira, A. (2006). Polarimetric and interferometric characterization of coherent scatterers in urban areas. *IEEE Transactions on Geoscience and Remote Sensing*, 44(4), 971–984. DOI: 10.1109/TGRS.2005.860950.